BIOCHEMISTRY
including biophysical chemistry & molecular biology

ARTICLE

pubs.acs.org/biochemistry

Enhancement of the Thermostability of *Hydrogenobacter thermophilus* Cytochrome c_{552} through Introduction of an Extra Methylene Group into Its Hydrophobic Protein Interior

Hulin Tai, Kiyofumi Irie, Shin-ichi Mikami, and Yasuhiko Yamamoto*

Department of Chemistry, University of Tsukuba, Tsukuba 305-8571, Japan

Supporting Information

ABSTRACT: Careful scrutiny of the protein interior of *Hydrogenobacter thermophilus* cytochrome c_{552} (HT) on the basis of its X-ray structure [Travaglini-Allocatelli, C., Gianni, S., Dubey, V. K., Borgia, A., Di Matteo, A., Bonivento, D., Cutruzzola, F., Bren, K. L., and Brunori, M. (2005) *J. Biol. Chem. 280*, 25729−25734] indicated that a void space, which is large enough to accommodate a methyl group, exists in the hydrophobic protein interior near the heme. We tried to reduce the void space through the replacement of a Val by Ile or Leu (Val/Ile or Val/Leu mutation), and then the structural and functional consequences of these two mutations were characterized in order to elucidate the relationship between the nature of the packing of hydrophobic residues and the functional properties of the protein. The study demonstrated striking differences in the structural and functional consequences between the two mutations. The Val/Ile mutation was found to cause further enhancement of the thermostability of the oxidized HT, as reflected in the increase of the denaturation temperature (T_m) value by ∼3 deg, whereas the thermostability of the reduced form was essentially unaffected. As a result, the redox potential (E_m) of the Val/Ile mutant exhibited a negative shift of ∼50 mV relative to that of the wild-type protein in an enthalpic manner, this being consistent with our previous finding that a protein with higher stability in its oxidized form exhibits a lower E_m value [Terui, N., Tachiiri, N., Matsuo, H., Hasegawa, J., Uchiyama, S., Kobayashi, Y., Igarashi, Y., Sambongi, Y., and Yamamoto, Y. (2003) *J. Am. Chem. Soc. 125*, 13650−13651]. In contrast, the Val/Leu mutation led to a decrease in thermostability of both the redox forms of the protein, as reflected in the decreases of the T_m values of the oxidized and reduced proteins by ∼3 and ∼5 deg, respectively, and the E_m value of the Val/Leu mutant happened to be similar to that of the Val/Ile one. The E_m value of the Val/Leu mutant could be reasonably interpreted in terms of the different effects of the mutation on the stabilities of the two different redox forms of the protein. Thus, the present study demonstrated that the stability of the protein is affected quite sensitively by the contextual stereochemical packing of hydrophobic residues in the protein interior and that the structural properties of the hydrophobic core in the protein interior are crucial for control of the redox function of the protein. These findings provide novel insights as to functional control of a protein, which could be utilized for tuning of the T_m and E_m values of the protein by means of protein engineering.

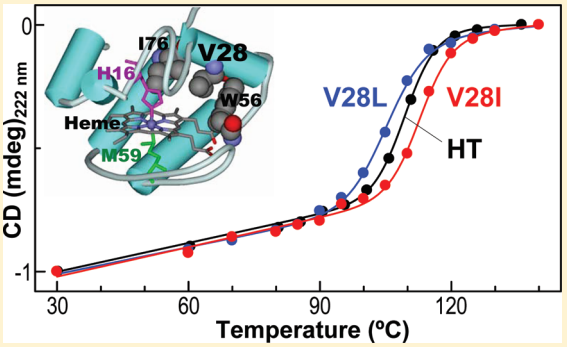

Understanding of the molecular basis of protein thermostabilitiy is an aim of immense fundamental and practical importance.[1,2] Comparative studies on the structures of homologous proteins from thermophiles and mesophiles have contributed significantly to understanding of the relationship between protein structure and thermostability.[3−15] In particular, studies on mutants of a mesophilic protein, of which amino acid substitutions were selected with reference to the corresponding residues in its thermophilic counterpart, have been quite effectively used to directly prove that specific interactions contribute to the high thermostability of thermophilic proteins.[2−5,13] Thermophile *Hydrogenobacter thermophilus* cytochrome c_{552} (HT) and mesophile *Pseudomonas aeruginosa* cytochrome c_{551} (PA) are monoheme-containing electron transfer proteins composed of 80 and 82 amino acid residues, respectively. Although the two proteins exhibit high sequence homology (56%),[14] and hence their main-chain folding is almost identical,[4,16,17] the denaturation temperatures (T_m) of the oxidized and reduced forms of HT are higher by ∼27 and ∼20 deg than those of the corresponding forms of PA, and the redox potential (E_m) of HT at pH 6.0 and 25 °C is lower by ∼60 mV relative to that of PA.[7,8,10] Mutants of PA, of which amino acid substitutions were selected with reference to the corresponding residues in HT in order to reinforce the hydrophobic protein interior, exhibited T_m and E_m values between those of the two proteins.[5−7] These studies clearly demonstrated not only that the contextual stereochemical

Received: February 18, 2011
Revised: March 18, 2011
Published: March 18, 2011

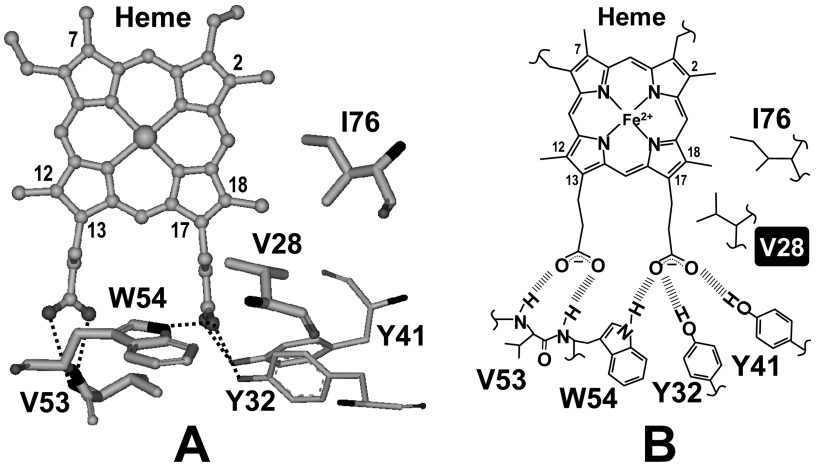

Figure 1. (A) Schematic representation of locations of amino acid residues V28, Y32, Y41, V53, W54, and I76 in the heme active site of *Hydrogenobacter thermophilus* cytochrome c_{552} (HT).[16] The amino acid residues are drawn as a stick model, and the heme as a ball and stick model. The hydrogen bonds between the residues and heme propionic acid side chains are denoted by broken lines. (B) Schematic drawing of the hydrogen bonds between the residues and heme propionic acid side chains. The hydrogen bonds are represented by bold gray broken lines.

packing of hydrophobic residues is crucial for the increased hydrophobic interaction conferring overall thermostability to proteins but also that the E_m value can be controlled through alteration of the protein stability. These findings have been successfully utilized to design and prepare HT mutants of which the T_m and E_m values are even higher and lower than the corresponding values of the wild-type protein, respectively.[18]

We further extended our efforts to control of the T_m and E_m values of HT through alteration of the packing of hydrophobic residues in the protein interior using amino acid substitutions. Careful scrutiny of the protein interior of HT on the basis of its X-ray structure[16] indicated that a void space, which is large enough to accommodate a methyl group, exists between the Val28 and Ile76 residues buried in the hydrophobic protein interior near the heme 17-propionic acid side chain (Figure 1A). The presence of such a void space possibly makes an unfavorable contribution to the stability of the protein interior. Consequently, the insertion of an extra CH_2 group into the Val28 side chain through a V28I or V28L mutation could possibly reduce the void space and hence reinforces the hydrophobic protein interior, leading to enhancement of the protein stability. Furthermore, Val28 is also located very close to Trp54, which plays a pivotal role in the noncovalent bond interaction between the heme and protein.[16] The Trp54 amide NH and $N_\varepsilon H$ hydrogen atoms are hydrogen-bonded to the carboxyl oxygen atoms of the heme 13- and 17-propionic acid side chains, respectively (Figure 1B).[16] The carboxyl oxygen atoms of the heme 13- and 17-propionic acid side chains also form hydrogen bonds with the Val53 amide NH hydrogen atom, and the Tyr32 and Tyr41 OH hydrogen atoms, respectively (Figure 1B).[16] Consequently, it is of fundamental interest to elucidate the effects of the V28I and V28L mutations on this heme−protein interaction and their functional consequences. Thus, this study was performed to provide detailed information as to the relationship between the nature of the contextual stereochemical packing of hydrophobic residues in the protein interior, and the structural and functional properties of the protein.

In the present study, we determine the influence of the introduction of an extra CH_2 group into the Val28 side chain buried in the hydrophobic protein interior of HT on the heme active site structure, and the T_m and E_m values of the protein through characterization of the V28I and V28L mutants in order to elucidate the relationship between the nature of the packing of hydrophobic residues and the functional properties of the protein. The study demonstrated striking differences in the structural and functional consequences between the two mutations. First, the V28I mutation caused further enhancement of the thermostability of the oxidized HT, as reflected in the increase of the T_m value by ~3 deg, whereas the thermostability of the reduced form was essentially unaffected. As expected from the observed effects of the V28I mutation on the thermostability of the two different redox forms of the protein, the E_m value of the V28I mutant exhibited a negative shift of ~50 mV relative to that of the wild-type protein in an enthalpic manner. These results were completely consistent with the previous finding that a protein with higher stability in its oxidized form exhibits a lower E_m value.[10,18] In contrast, the V28L mutation led to a decrease in thermostability of both the redox forms of the protein, as reflected in the decreases of the T_m values of the oxidized and reduced proteins by ~3 and ~5 deg, respectively, and the E_m value of the V28L mutant happened to be similar to that of the V28I one. The E_m value of the V28L mutant could be reasonably interpreted in terms of the different effects of the mutation on the stabilities of the oxidized and reduced forms of the protein. Thus, the present study demonstrated that the stability of the protein is affected quite sensitively by the contextual stereochemical packing of hydrophobic residues in the protein interior and that the structural properties of the hydrophobic core in the protein interior are crucial for control of the redox function of the protein.

MATERIALS AND METHODS

Protein Samples. The wild-type HT and its mutants were produced using *Escherichia coli* and purified as reported previously.[5,6] The oxidized forms of the proteins were prepared by the addition of a 10-fold molar excess of potassium ferricyanide. For NMR samples, the proteins were concentrated to about 1 mM in an ultrafiltration cell (YM-5, Amicon), and then 10% ^2H_2O or 100% ^2H_2O was added to the protein solutions. The pH of each sample was adjusted using 0.2 M KOH or 0.2 M HCl and

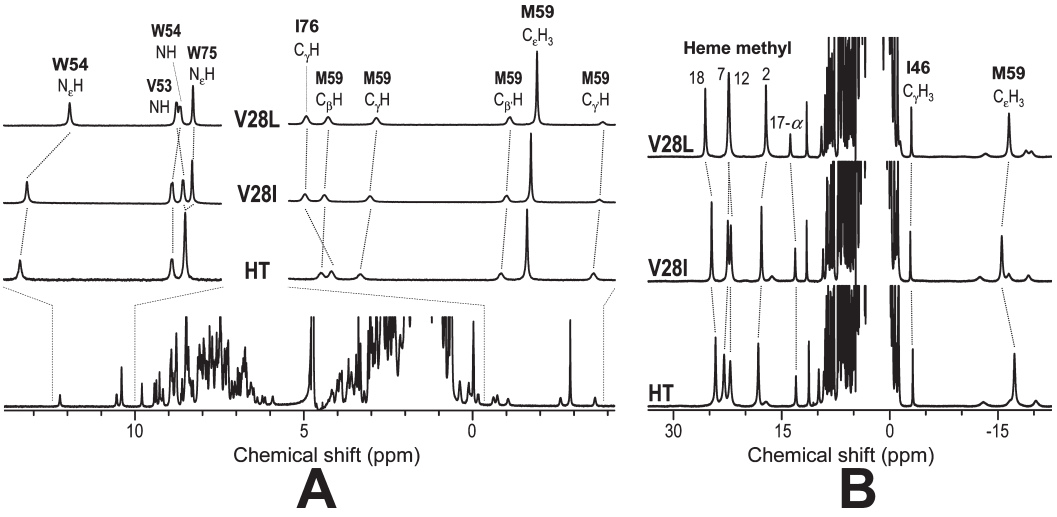

Figure 2. (A) 600 MHz ^{1}H NMR spectrum of the reduced form of the wild-type HT in 90% H_2O/10% ^2H_2O, pH 7.0, at 25 °C, and portions of the spectrum (−4 to −0.5 ppm and 10−12.3 ppm), together with corresponding ones of the reduced forms of V28I and V28L mutants under identical solution conditions, is expanded in the inset. (B) 600 MHz ^{1}H NMR spectra of the oxidized forms of the three proteins in 100% ^2H_2O, pH 7.0, at 25 °C. The assignments of some signals are indicated in the spectra, and the corresponding resonances are connected by broken lines.

was monitored with a Horiba F-22 pH meter with a Horiba type 6069-10C electrode.

Cyclic Voltammetry (CV). The procedures used for obtaining cyclic voltammograms for the proteins were essentially the same as those described previously.[19,20] CV experiments were performed with a Potentiostat-Galvanostat PGSTAT12 (Autolab, Netherland). A glassy carbon electrode (GCE) was polished with a 0.05 μm alumina slurry and then sonicated in deionized water for 1 min. Two microliters of a 1 mM protein solution was spread evenly with a microsyringe onto the surface of the GCE. Then the GCE surface was covered with a semipermeable membrane. All redox potentials (E_m) were referenced to a standard hydrogen electrode (SHE). The experimental error for E_m was ± 2 mV. Variable temperature experiments were performed using a home-built non-isothermal electrochemical cell configuration,[21] in which the temperature of the reference electrode was kept constant. The anodic to cathodic peak current ratios obtained at various potential scan rates (1−100 mV s^{-1}) were all ∼1. Both the anodic and cathodic peak currents increased linearly as a function of the square root of the scan rate in the range up to 100 mV s^{-1}. Thus, HT and its mutants exhibit quasi-reversible redox processes.

^{1}H NMR. NMR spectra were recorded on a Bruker Avance 600 FT NMR spectrometer operating at the ^{1}H frequency of 600 MHz. The signal assignments were based on two-dimensional double quantum-filtered chemical shift correlation spectroscopy (DQF-COSY), total COSY (TOCSY), and nuclear Overhauser effect correlated spectroscopy (NOESY) spectra acquired using the standard pulse sequences. To detect connectivities between paramagnetically shifted signals, NOESY spectra with a spectral width of 60 ppm in the t_1 and t_2 dimensions, with 512 and 4096 complex points in the t_1 and t_2 dimensions, respectively, were acquired. To optimize the detection of connectivities in the region of about −5.0 to 15 ppm (−25 to 35 ppm), two-dimensional spectra of the reduced (oxidized) proteins were acquired with a spectral width of 20 ppm (60 ppm) and 4096 complex points in both dimensions, respectively. TOCSY spectra were obtained with a mixing time of 10 or 200 ms, and NOESY spectra with a mixing time of 100 or 200 ms. Before Fourier transformation, a phase-shifted sine-squared window function was applied to both dimensions. Water suppression was performed by the presaturation method or watergate method.[22] Chemical shifts are given in ppm downfield from sodium 2,2-dimethyl-2-silapentane-5-sulfonate with H_2O as an internal reference.

Circular Dichroism Spectroscopy. CD spectra were recorded on a JASCO J-820 spectrometer over the spectral range of 200 to 250 nm and in the temperature range of 30−160 °C, using an airtight pressure proof cell compartment with quartz windows, which was described previously.[11]

RESULTS

^{1}H NMR Spectra of the Mutants. We first analyzed the effects of the mutations on the heme active site structure of the protein by means of ^{1}H NMR (Figure 2). In the ^{1}H NMR spectrum of the reduced protein, several signals had shifted outside the diamagnetic envelope due to porphyrin ring-current shifts or a deshielding effect of an intramolecular hydrogen bond (Figure 2A). The upfield-shifted Met59 proton signals were slightly affected by the mutations, suggesting subtle differences in the orientation of the Met59 side chain protons with respect to the heme porphyrin ring among the proteins. Furthermore, the downfield shift changes of ∼0.3 ppm for the Ile76 $C_\gamma H$ proton signals of the mutants, relative to that of the wild-type protein, could be attributed to the decreases in their porphyrin ring-current shifts. Since the side chains of Ile76 and V28 are in contact with each other[16] (Figure 1A), the insertion of an extra CH_2 group into the side chain of Val28 through a V28I or V28L mutation could result in displacement of the Ile76 side chain away from the porphyrin ring of the heme, leading to reduction of their upfield shifts in the porphyrin ring-current. In addition, the Trp54 amide NH and $N_\varepsilon H$ proton signals observed at 10.54 and 12.22 ppm, respectively, in the spectrum of the wild-type protein exhibited upfield shift changes of 0.01 and 0.08 ppm, respectively, upon the V28I mutation, and ones of 0.04 and 0.59 ppm, respectively, upon the V28L mutation. In contrast to the Trp54 NH proton signals, the Val53 amide NH proton signal exhibited slight downfield shift changes upon the mutations. Finally, the shifts of most heme peripheral side chain proton

dx.doi.org/10.1021/bi200256d |*Biochemistry* 2011, 50, 3161–3169

Table 1. Chemical Shifts (ppm) of Heme Side Chain ^{1}H NMR Signals of the Wild-Type HT, and V28I and V28L Mutants at pH 7.0 and 25 °C

	Reduced Form											
	18-Me	12-Me	7-Me	2-Me	3-H_α	3-Me_β	8-H_α	8-Me_β	5-H	10-H	15-H	20-H
HT	3.44	3.31	2.43	1.99	6.14	3.67	6.22	3.86	9.78	9.42	9.36	9.27
V28I	3.40	3.29	2.40	1.97	6.12	3.67	6.19	3.83	9.73	9.38	9.30	9.23
V28L	3.28	3.31	2.39	1.97	6.11	3.64	6.22	3.83	9.73	9.45	9.32	9.19

	Oxidized Form									
					propionic acid side chain					
	18-Me	12-Me	7-Me	2-Me	17-H_α	17-$H_{\alpha'}$	$\Delta\delta_\alpha$[a]	13-H_α	13-$H_{\alpha'}$	$\Delta\delta_\alpha$[a]
HT	24.15	22.96	22.14	18.21	13.03	2.09	11.81	9.17	3.64	5.53
V28I	24.75	22.48	22.07	17.81	13.14	3.19	9.95	8.49	3.40	5.09
V28L	25.60	22.30	22.38	17.17	13.81	4.55	9.26	8.15	2.99	5.16

[a] The difference between H_α and $H_{\alpha'}$ proton shifts.

signals were affected very little by the mutations, the exception being the heme 18-methyl proton signal, which exhibited upfield shift changes of 0.16 ppm upon the mutations (Table 1).

In the spectra of the oxidized proteins, paramagnetically shifted signals arising from the Fe-coordinated Met59 side chain and Ile46 $C_{\gamma'}H_3$ protons, and heme peripheral methyl ones were resolved in upfield and downfield shifted regions, respectively (Figure 2B). These signals have been shown to be sensitive to the heme environment.[23−25] The Met59 $C_\varepsilon H_3$ proton signal exhibited relatively large downfield-shifts of 1.54 and 0.94 ppm with the V28I and V28L mutations, respectively. Since the shift of the Ile46 $C_{\gamma'}H_3$ proton signal was only slightly affected by the mutations, the observed shift changes of the Met59 $C_\varepsilon H_3$ proton signal are likely to be due to a local structural alteration induced by the mutations, possibly a subtle conformational alteration of the Met59 side chain relative to the heme (see below). Among the assigned heme proton signals of the oxidized proteins, the heme methyl proton signals exhibited relatively large mutation-induced shift changes (Table 1), suggesting that the heme electronic structure is affected by the mutations. Furthermore, the large mutation-induced shift changes observed for the heme propionic acid α-CH_2 proton signals also suggested that the conformation of the heme propionate side chains is affected by the mutations (see below).

Thermostabilities of the Mutants. We next analyzed the thermostabilities of the oxidized and reduced forms of the mutants at pH 7.0 through measurement of CD spectra (200−250 nm) in the temperature range of 30−160 °C (Supporting Information). The fractions of the unfolded proteins calculated from the CD ellipticity at 222 nm were plotted against temperature, thermal unfolding profiles for the two mutants in both redox forms being obtained (Figure 3). Similar plots for the wild-type protein are also illustrated, for comparison, in Figure 3. The T_m values of the oxidized and reduced V28I mutant were determined to be 113.2 and 129.9 °C, respectively, and those of the oxidized and reduced V28L one to be 106.6 and 124.4 °C, respectively (Table 2). Comparison of the T_m value between the mutant and wild-type proteins showed that the V28I mutation increases the thermostability of the oxidized protein, as reflected in the elevation of the T_m value by ∼3 deg, whereas that of the reduced protein is essentially unaffected by the mutation. On the other hand, the V28L mutation decreases the thermostabilities of

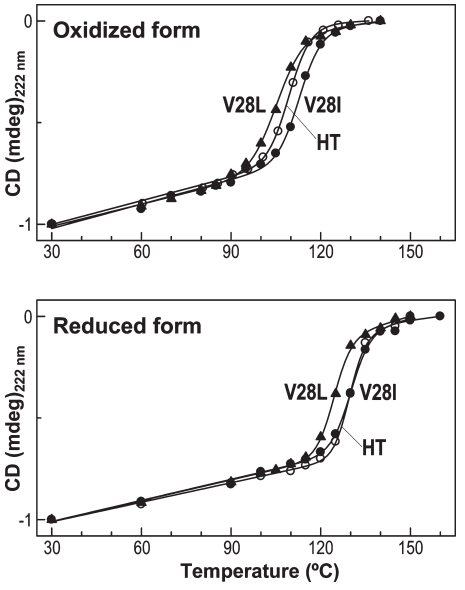

Figure 3. Thermal unfolding profiles of the oxidized (top) and reduced (bottom) forms of the wild-type HT (○), and V28I (●) and V28L (▲) mutants at pH 7.0.

both the oxidized and reduced proteins, as reflected in the decreases of the T_m values of the oxidized and reduced proteins by ∼3 and ∼5 deg, respectively.

The thermostabilities of the heme active site structures of the oxidized proteins were also analyzed through measurement of ^{1}H NMR spectra at various temperatures (Supporting Information). The heme methyl and Met59 proton signals of the oxidized V28I and V28L mutants could be observed up to 86 °C (Supporting Information), reflecting the thermostabilities of their heme active sites. Similar to the case of the wild-type protein, the heme methyl and axial Met59 proton signals of the oxidized V28I and V28L mutants exhibited anomalous line-broadening at low temperatures due to a dynamic structure transition of the heme active site (Supporting Information).[20]

pH Profiles of the E_m Values of the Mutants. We also measured the E_m values of the mutants at various pHs (Supporting Information). The pH profiles of the E_m values of

Table 2. Denaturation Temperature and Thermodynamic Parameters of the Redox Reaction for the Wild-Type HT, and V28I and V28L Mutants

	T_m (°C)[a]				ΔH (kJ mol^{-1})[d]		ΔS (J K^{-1} mol^{-1})[d]	
	oxidized	reduced	ΔT_m (°C)[b]	E_m (mV)[c]	low	high	low	high
HT	109.8[e](−)[f]	129.7[e](−)[f]	19.9	245[g]	−32.2[g]	−37.5[g]	−28.4[g]	−45.7[g]
V28I	113.2 (+3.4)[f]	129.9 (+0.2)[f]	16.7	199	−26.0	−29.0	−22.6	−32.5
V28L	106.6 (−3.2)[f]	124.4 (−5.3)[f]	17.8	196	−26.1	−29.7	−23.7	−35.7

[a] Denaturation temperature determined through analysis of the temperature dependence of the CD ellipticity at 222 nm and pH 7.0. The experimental error was ± 0.2 °C. [b] The difference in T_m value between the reduced and oxidized forms of the protein. [c] Redox potential determined at pH 6.0 and 25 °C. The experimental error was ± 2 mV. [d] Entropic and enthalpic contributions to the E_m value at pH 6.0. The experimental errors for ΔH and ΔS of the proteins were ± 2 kJ mol^{-1} and ± 3 J K^{-1} mol^{-1}, respectively. [e] Cited from ref 11. [f] The numbers in parentheses indicate the change in the T_m value relative to that of the wild-type HT. [g] Cited from ref 18.

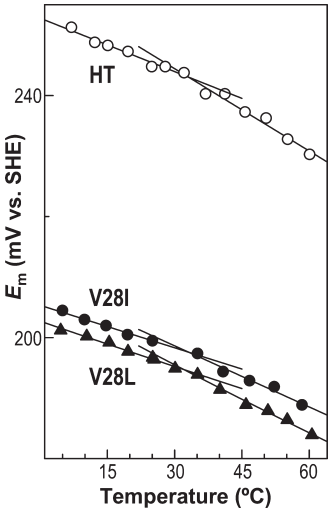

Figure 4. Plots of the redox potentials (E_m) against temperature for the wild-type HT (○), and V28I (●) and V28L (▲) mutants at pH 6.0. The plots for the proteins could be fitted by two straight lines with a transition temperature of ∼35 °C, and hence two sets of thermodynamic parameters for the E_m value were obtained, as shown in Table 2.

the mutants were highly similar to each other and were also quite similar in pattern to that of the wild-type protein, the exception being the negative shifts of ∼50 mV for the mutants relative to that of the wild-type protein throughout the pH range examined (Table 2). The negative shift of the E_m value of the V28I mutant relative to that of the wild-type protein is consistent with our previous finding that a protein with higher stability in its oxidized form exhibits a lower E_m value.[10,12,18] On the other hand, the E_m value of the V28L mutant happened to be almost equal to that of the V28I one, although the thermostability of the former mutant is distinctly lower than that of the latter. This finding could be interpreted in terms of the difference in the effect of the V28L mutation on stability between the two redox forms of the protein (see below).

Temperature Dependence of the E_m Values of the Mutants. We finally measured the E_m values of the mutants at various temperatures, and the obtained values, together with those of the wild-type protein for comparison, are plotted against temperature (E_m-T plots) in Figure 4. From the E_m-T plots, we estimated the enthalpic (ΔH) and entropic (ΔS) contributions to the E_m value (Table 2). The plots for the proteins could be fitted by two straight lines with a transition temperature (T_c) of ∼35 °C [15,18,20,26] (Figure 4). Hence, two sets of values, $\Delta H^{(Low)}$ and $\Delta S^{(Low)}$, and $\Delta H^{(High)}$ and $\Delta S^{(High)}$, in the temperature ranges of $< T_c$ and $> T_c$, respectively, were determined for these proteins (Table 2). The anomalous line-broadening of the ^{1}H NMR signals arising from the heme methyl and Met59 protons of the HT proteins at low temperatures has been attributed to a temperature-dependent conformational transition between two different protein structures, which slightly differ in the conformation of the loop bearing the Met59 residue.[20] Hence, the appearance of the two different protein structures exhibiting distinctly different thermodynamic parameters resulted in the two sets of thermodynamic parameters for the protein. Not only the absolute $\Delta H^{(Low)}$ and $\Delta H^{(High)}$ values but also the absolute $\Delta S^{(Low)}$ and $\Delta S^{(High)}$ ones determined for the mutants were smaller than the corresponding values of the wild-type protein. Hence, the observed negative shifts of the E_m value caused by the mutations indicated that the enthalpic contribution prevails over the entropic one in E_m control.

DISCUSSION

Effects of the Mutations on the Heme Active Site Structure. The effects of the mutations on the structure of HT were manifested in the shift changes of the ^{1}H NMR signals in the spectra of both the reduced and oxidized proteins. The Ile76 $C_\gamma H$ proton signal of the reduced protein exhibited downfield shifts of ∼0.3 ppm upon the two mutations (Figure 2A), indicating sizable displacement of this residue away from the heme due to the steric hindrance with the contact between the side chains of Ile76 and the 28th residue in the mutant proteins. In addition, the Trp54 amide NH and $N_\varepsilon H$ proton signals exhibited relatively large mutation-induced shift changes, which could be interpreted in terms of the effects of the mutations on the hydrogen bonding interactions associated with these NH protons. The Trp54 amide NH and $N_\varepsilon H$ protons are hydrogen-bonded to the carboxyl oxygen atoms of the heme 13- and 17-propionic acid side chains, respectively, and the other carboxyl oxygen atom of the heme 13-propionic acid side chain also accepts the Val53 amide NH hydrogen atom to form a hydrogen bond (Figure 1B). The upfield shift changes of the Trp54 amide NH and $N_\varepsilon H$ proton signals upon the mutations are most likely due to weakening of the hydrogen bonds between the Trp54 and heme propionic acid side chains (Trp54-heme hydrogen bonds). Since the Trp54 NH proton signals of the V28L mutant exhibited larger mutation-induced shift changes than those of the V28I one, the Trp54-heme hydrogen bonds in the former mutant

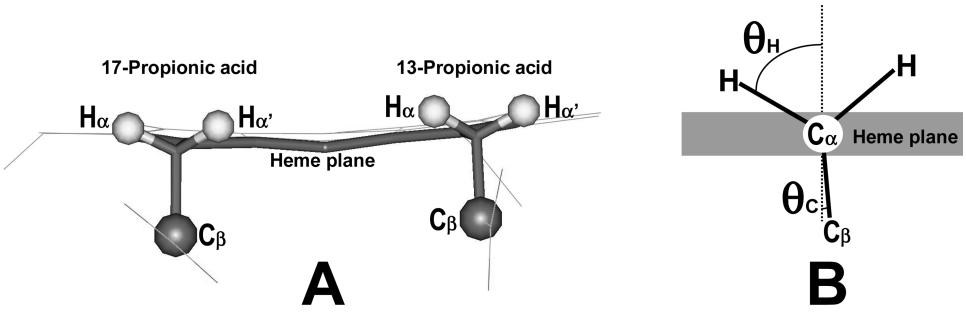

Figure 5. (A) Orientation of the heme 13- and 17-propionic acid α-CH_2 groups with respect to the heme in the active site of *Hydrogenobacter thermophilus* cytochrome c_{552} (HT).[16] (B) The orientation of the heme propionic acid side chain α-CH_2 hydrogen (C_β carbon) atom with respect to the heme plane is defined by the dihedral angle θ_H (θ_C) between the C_α-H (C_α-C_β) vector and the normal to the heme plane, which is illustrated as a dotted line.

appeared to be more significantly weakened than those in the latter. In contrast to the Trp54 NH proton signals, the Val53 amide NH proton signal of the protein exhibited slight downfield shift changes upon the mutations, indicative of slight strengthening of the hydrogen bond between Val53 and heme 13-propionic acid side chains. Thus, the Trp54-heme hydrogen bonds were found to be affected by the stereochemical packing around the 28th residue. Finally, despite these local and subtle structural changes induced by the mutations, the overall protein structures of the V28I and V28L mutants were quite similar to that of the wild-type protein, as reflected in the similarity in the Ile46 $C_{\gamma'}H_3$ proton shifts among the oxidized proteins (Figure 2B).

The effects of the mutations on the heme active site structure could be characterized in detail through analysis of the shifts of the ^{1}H NMR signals of the oxidized proteins. First, the large downfield shift changes observed for the Met59 $C_\varepsilon H_3$ proton signal of the oxidized protein upon the mutations could be accounted for by a subtle change in the Met59 side chain conformation. The Met59 $C_\varepsilon H_3$ proton is located at 0.36 nm from the heme Fe atom,[16] and hence its shift is extremely sensitive to its orientation with respect to the heme. Assuming that the mutation-induced shift change for the Met59 $C_\varepsilon H_3$ proton signal is solely due to a paramagnetic pseudocontact shift contribution, the conformational change of the Met59 side chain could be inferred from the shift analysis involving the previously determined principal axes of the paramagnetic susceptibility tensor in the oxidized HT.[27] The paramagnetic pseudocontact shift for the Met59 $C_\varepsilon H_3$ proton signal depends upon the orientation of the vector between the heme Fe atom and the center of gravity of the Met59 $C_\varepsilon H_3$ hydrogen atoms (Fe-Met59 $C_\varepsilon H_3$ vector), with respect to the principal magnetic axes. The analysis indicated that a change of a few degrees in the angle between the Fe-Met59 $C_\varepsilon H_3$ vector and the z axis of the tensor accounts for the observed shift changes. Such an alteration of the Met59 coordination structure induced by the mutations could also account, to some extent, for the mutation-induced shift changes observed for the heme methyl and propionic acid side chain proton signals of the oxidized protein, because the coordination structure of the Met59 side chain is the main determinant of control of the delocalization pattern of an unpaired electron from the heme iron atom toward the porphyrin π-system, which predominantly determines the paramagnetic shifts of the heme peripheral side chain proton signals.[27−29] Thus, the coordination structure of the Met59 side chain as to the heme Fe atom was found to be slightly affected by the V28I and V28L mutations. Furthermore, the small mutation-induced shift change of the Met59 proton signal of the reduced protein, that is, 0.08 ppm, also supported a subtle change in the conformation of the Met59 side chain.

We next analyzed the effects of the mutations on the conformation of the heme propionic acid side chains through analysis of the α-CH_2 proton shifts of the oxidized proteins. The paramagnetic shift of a heme propionic acid side chain α-CH_2 proton signal is extremely sensitive to the orientation of the CH_2 group relative to the heme plane. Its paramagnetic contact shift is approximately proportional to the quantity $\rho \times \cos^2 \theta_H$, where ρ and θ_H represent the unpaired electron density in the p_z orbital of a pyrrole carbon atom to which the CH_2 group is covalently attached, and the dihedral angle between the CH vector and the normal to the heme plane, respectively[24,30] (Figure 5). Hence, roughly speaking, the difference in the shift between the α-CH_2 proton signals ($\Delta\delta_\alpha$) reflects its orientation with respect to the heme plane. According to the X-ray structural data for the wild-type HT,[16] four HT molecules are accommodated in an asymmetric unit of a protein crystal, and average θ_C values of ∼4° and ∼7° were calculated for the values for the heme 13- and 17-propionic acid side chains, respectively, where the θ_C value is defined as the dihedral angle between the C_α-C_β vector and the normal to the heme plane (Figure 5). Therefore, the $\Delta\delta_\alpha$ values of 5.53 and 10.94 ppm for the heme 13- and 17-propionic acid side α-CH_2 groups, respectively (Table 1), were roughly consistent with the smaller θ_C value for the former than the latter. By the way, the shifts of the heme 13-propionic acid α-CH_2 proton signals of the oxidized protein were affected by the mutations due to the slight mutation-induced alteration of the heme electronic structure, as reflected in the slight shift changes of the heme methyl proton signals (Table 1). The shifts of heme propionic acid α-CH_2 proton signals are altered through a change in the ρ value as a result of alteration of the heme electronic structure. Despite the relatively large shift changes for the α-CH_2 proton signals, the $\Delta\delta_\alpha$ values for the heme 13-propionic acid side chains of the mutant proteins, that is, 5.09 and 5.16 ppm for the V28I and V28L mutants, respectively, were similar to that of the wild-type protein, that is, 5.53 ppm. These results suggested that the θ_C value of the heme 13-propionic acid side chain is only slightly, if any, affected by the mutations. In contrast, the $\Delta\delta_\alpha$ value for the heme 17-propionic acid side chain was greatly altered by the mutations, that is, 11.81, 9.95, and 9.26 ppm for HT, V28I, and V28L, respectively, suggesting that the θ_C value of the heme 17-propionic acid side chain of the protein is greatly affected by the mutations. The mutation-induced change of the heme 17-propionic acid side chain conformation could be due to that of the Trp54-heme hydrogen bonds, as reflected in the shift changes of

the Trp54 NH proton signals. Thus, the insertion of an extra CH_2 group into the Val28 side chain through the mutations was found to result in local and subtle structural changes in the heme active site of the protein.

Effects of the Mutations on Protein Stability. In spite of the structural similarity among the mutant and wild-type proteins, the thermostability of the protein was affected by the mutations. The T_m value of the oxidized V28I mutant was higher by ~3 deg relative to that of the oxidized wild-type protein, whereas those of the reduced forms of the two proteins were almost identical to each other. This finding is consistent with our previous one that, upon reinforcement of the hydrophobic protein interior through reduction of the void space by means of amino acid replacements, an oxidized protein is more greatly stabilized than its reduced form.[10,18] In contrast, the V28L mutation resulted in decreases in the thermostability of not only the oxidized protein, but also, and even more significantly, the reduced one, as reflected in the decreases of the T_m values by ~3 and ~5 degrees, respectively. Hence, the V28L mutation was different from the other mutations in terms of its effects on the thermostabilities of the two different redox forms of the protein.

The decrease in the protein thermostability upon the V28L mutation could be attributed to a structural alteration that causes weakening of the Trp54-heme hydrogen bonds, as reflected in the mutation-induced shift changes of the Trp54 NH proton signals (see above). Since weakening of the Trp54-heme hydrogen bonds is thought to arise from an unfavorable steric interaction among Trp54, Ile76, heme 17-propionic acid, and introduced Leu28 side chain in the V28L mutant, the stereochemical packing of hydrophobic residues in the protein interior of this mutant is likely to be inferior to that in the wild-type protein. Hence, such an unfavorable steric interaction in the protein interior of the V28L mutant decreased the stability of the highly stable reduced protein to a greater extent, compared with that of the less stable oxidized one. The observed difference in the thermostability between the V28I and V28L mutant proteins demonstrated that the overall protein stability is quite sensitively affected by the nature of the contextual stereochemical packing of hydrophobic residues in the protein interior.

Relationship between Redox Function and Protein Stability. We demonstrated previously that the E_m value of a protein is controlled through the protein stability.[10,12] In the case of the V28I mutation, as reflected in the elevation by ~3 deg of the T_m value of the oxidized V28I relative to that of the oxidized HT (Table 2), the oxidized protein was stabilized by the mutation, whereas the stability of the reduced protein was essentially unaffected by the mutation. Consequently, as expected from the increased stability, the V28I mutant exhibited a negative shift of ~50 mV relative to that of the wild-type protein, this being consistent with our previous finding that a protein with higher stability exhibits a lower E_m value.[10,12,18] On the other hand, the E_m value of the V28L mutant exhibited a similar negative shift of ~50 mV relative to that of the wild-type protein, although the stability of this mutant was lower than that of the wild-type one.

The E_m values of the V28I and V28L mutants could be interpreted in terms of the effects of the mutations on the thermostabilities of the oxidized and reduced proteins. The E_m value of a protein is determined by the difference in thermodynamic stability between the two redox forms. Since the T_m value of a protein may be considered as a semiquantitative index for its thermodynamic stability, the difference in the T_m value between the two redox forms of a protein (ΔT_m) could be used as a semiquantitative measure of the difference in thermodynamic stability between them. ΔT_m values of 19.9, 16.7 and 17.8 deg were calculated for the wild-type HT, and V28I and V28L mutant proteins, respectively, and the calculated ΔT_m values of the proteins correlated fairly well with their E_m values. This interpretation was supported by the results of thermodynamic analysis of the E_m values, which demonstrated not only that the ~50 mV negative shifts of the E_m values of the mutants relative to that of the wild-type protein are enthalpic in origin, but also that the ΔH contributions of the V28I and V28L mutants are almost identical to each other (Table 2).

Furthermore, thermodynamic analysis of the E_m values indicated that the absolute ΔS value ($|\Delta S|$) was decreased by the V28I and V28L mutations. These results were in sharp contrast to those for the mutations previously examined, which resulted in either the same or an increased absolute ΔS value.[10,15,18,26,31] The internal mobility of a protein has been shown to play a crucial role in ΔS control.[32] The reinforcement of the hydrophobic protein interior through reduction of the void space by the V28I mutation is likely to decrease the entropy of the protein through suppression of its internal mobility. Hence, the entropy of the oxidized protein exhibiting intrinsically greater internal mobility is expected to be more significantly reduced by the mutation than that of the reduced form, leading to a decrease in the $|\Delta S|$ value, as observed in the study. On the other hand, the smaller $|\Delta S|$ values for the V28L mutant, compared with the corresponding ones for the wild-type HT, might be attributed to the redox-dependent effects of the mutation on the internal mobility of the protein. The unfavorable steric interaction among the introduced Leu28, nearby amino acid and heme 17-propionic acid side chains in the V28L mutant is expected to result in an increase in the internal mobility of both the reduced and oxidized proteins. As reflected in the greater decrease of the T_m value for the reduced form of the V28L mutant than the oxidized one, relative to those for the corresponding redox forms of the wild-type HT, the increase in the internal mobility of the reduced mutant appeared to be larger than that in the oxidized one, leading to a decrease in the $|\Delta S|$ value. Although it has been proposed that a redox-dependent solvent reorganization effect plays a significant role in the ΔS control of proteins,[33−35] it is not clear at present if there is a sizable difference in solvent accessibility among the proteins.

CONCLUDING REMARKS

The influence of the introduction of an extra CH_2 group into the Val28 side chain buried in the hydrophobic protein interior of HT on the heme active site structure, and the T_m and E_m values of the protein have been determined through characterization of the V28I and V28L mutants in order to elucidate the relationship between the nature of the packing of hydrophobic residues and the functional properties of the protein. Despite the structural similarity among the mutant and wild-type proteins, the mutants exhibited distinctly different T_m and E_m values from those of the wild-type protein. Although the E_m values of the mutants were very similar to each other, thermodynamic analysis of their E_m values revealed a distinct difference in the ΔS contribution between them. Thus, the present study demonstrated a remarkably large effect of the introduction of an extra CH_2 group on the functional properties of the protein. This finding provides novel insights as to functional control of a protein, which could be utilized for tuning of the T_m and E_m values of the protein by means of protein engineering.

■ ASSOCIATED CONTENT

Supporting Information. Temperature-dependence of 600 MHz ^{1}H NMR spectra of the oxidized forms of HT, V28I, and V28L in 90% H_2O/10% ^2H_2O, pH 7.0, temperature-dependence of CD spectra, 200−250 nm, of the oxidized and reduced forms of V28I and V28L at pH 7.0, and plots of the redox potentials (E_m) against pH for the wild-type HT, and V28I and V28L mutants at 25 °C. This material is available free of charge via the Internet at http://pubs.acs.org.

■ AUTHOR INFORMATION

Corresponding Author

*Phone and Fax: +81-29-853-6521. E-mail: yamamoto@chem.tsukuba.ac.jp

Funding Sources

This work was supported by a Grant-in-Aid for Scientific Research on Innovative Areas (No. 21108505, "π-Space") from the Ministry of Education, Culture, Sports, Science and Technology, Japan, the Yazaki Memorial Foundation for Science and Technology, and the NOVARTIS Foundation (Japan) for the Promotion of Science.

■ ACKNOWLEDGMENT

The ^{1}H NMR spectra were recorded on a Bruker AVANCE-600 spectrometer at the Chemical Analysis Center, University of Tsukuba.

■ ABBREVIATIONS USED

E_m, redox potential; cyt *c*, cytochrome *c*; T_m, denaturation temperature of protein; DQF-COSY, two-dimensional double quantum-filtered chemical shift correlation spectroscopy; TOCSY, total COSY; NOESY, two-dimensional nuclear Overhauser effect-correlated spectroscopy; T_c, transition temperature; CV, cyclic voltammetry; E_m−pH plots, plots of redox potentials of proteins against pH; E_m−*T* plots, plots of redox potentials of proteins against temperature

■ REFERENCES

(1) Vinther, J. M., Kristensen, S. M., and Led, J. J. (2010) Enhanced stability of a protein with increasing temperature. *J. Am. Chem. Soc. 133*, 271–278.

(2) Atomi, H. (2005) Recent progress toward the application of hyperthermophiles and their enzymes. *Curr. Opin. Chem. Biol. 9*, 166–173.

(3) Cambillau, C., and Claverie, J. (2000) Structural and genomic correlates of hyperthermostability. *J. Biol. Chem. 275*, 32383–32386 and references therein.

(4) Hasegawa, J., Yoshida, T., Yamazaki, T., Sambongi, Y., Yu, Y., Igarashi, Y., Kodama, T., Yamazaki, K., Kyogoku, Y., and Kobayashi, Y. (1998) Solution structure of thermostable cytochrome *c*-552 from *Hydrogenobacter thermophilus* determined by ^{1}H-NMR spectroscopy. *Biochemistry 37*, 9641–9649.

(5) Hasegawa, J., Shimahara, H., Mizutani, M., Uchiyama, S., Arai, H., Ishii, M., Kobayashi, Y., Ferguson, S. J., Sambongi, Y., and Igarashi, Y. (1999) Stabilization of *Pseudomonas aeruginosa* cytochrome c_{551} by systematic amino acid substitutions based on the structure of thermophilic *Hydrogenobacter thermophilus* cytochrome c_{552}. *J. Biol. Chem. 274*, 37533–37537.

(6) Hasegawa, J., Uchiyama, S., Tanimoto, Y., Mizutani, M., Kobayashi, Y., Sambongi, Y., and Igarashi, Y. (2000) Selected mutations in a mesophilic cytochrome *c* confer the stability of a thermophilic counterpart. *J. Biol. Chem. 275*, 37824–37828.

(7) Uchiyama, S., Hasegawa, J., Tanimoto, Y., Moriguchi, H., Mizutani, M., Igarashi, Y., Sambongi, Y., and Kobayashi, Y. (2002) Thermodynamic characterization of variants of mesophilic cytochrome *c* and its thermophilic counterpart. *Protein Eng. 15*, 455–461.

(8) Sambongi, Y., Uchiyama, S., Kobayashi, Y., Igarashi, Y., and Hasegawa, J. (2002) Cytochrome *c* from a thermophilic bacterium has provided insights into the mechanisms of protein maturation, folding, and stability. *Eur. J. Biochem. 269*, 3355–3361.

(9) Yamamoto, Y., Terui, N., Tachiiri, N., Minakawa, K., Matsuo, H., Kameda, T., Hasegawa, J., Sambongi, Y., Uchiyama, S., Kobayashi, Y., and Igarashi, Y. (2002) Influence of amino acid side chain packing on Fe-methionine coordination in thermostable cytochrome *c*. *J. Am. Chem. Soc. 124*, 11574–11575.

(10) Terui, N., Tachiiri, N., Matsuo, H., Hasegawa, J., Uchiyama, S., Kobayashi, Y., Igarashi, Y., Sambongi, Y., and Yamamoto, Y. (2003) Relationship between redox function and protein stability of cytochromes *c*. *J. Am. Chem. Soc. 125*, 13650–13651.

(11) Uchiyama, S., Ohshima, A., Nakamura, S., Hasegawa, J., Terui, N., Takayama, S. J., Yamamoto, Y., Sambongi, Y., and Kobayashi, Y. (2004) Complete thermal-unfolding profiles of oxidized and reduced cytochromes *c*. *J. Am. Chem. Soc. 126*, 14684–14685.

(12) Takayama, S. J., Mikami, S., Terui, N., Mita, H., Hasegawa, J., Sambongi, Y., and Yamamoto, Y. (2005) Control of the redox potential of *Pseudomonas aeruginosa* cytochrome c_{551} through the Fe-Met coordination bond strength and pK_a of a buried heme propionic acid side chain. *Biochemistry 44*, 5488–5494.

(13) Oikawa, K., Nakamura, S., Sonoyama, T., Ohshima, A., Kobayashi, Y., Takayama, S. J., Yamamoto, Y., Uchiyama, S., Hasegawa, J., and Sambongi, Y. (2005) Five amino acid residues responsible for the high stability of *Hydrogenobacter thermophilus* cytochrome c_{552}. *J. Biol. Chem. 280*, 5527–5532.

(14) Sanbongi, Y., Ishii, M., Igarashi, Y., and Kodama, T. (1989) Amino acid sequence of cytochrome c-552 from a thermophilic hydrogen-oxidizing bacterium, *Hydrogenobacter thermophilus*. *J. Bacteriol. 171*, 65–69.

(15) Takahashi, Y., Takayama, S. J., Mikami, S., Mita, H., Sambongi, Y., and Yamamoto, Y. (2006) Influence of a single amide group on the redox function of *Pseudomonas aeruginosa* cytochrome c_{551}. *Chem. Lett. 35*, 528–529.

(16) Travaglini-Allocatelli, C., Gianni, S., Dubey, V. K., Borgia, A., Di Matteo, A., Bonivento, D., Cutruzzola, F., Bren, K. L., and Brunori, M. (2005) An obligatory intermediate in the folding pathway of cytochrome c_{552} from *Hydrogenobacter thermophilus*. *J. Biol. Chem. 280*, 25729–25734.

(17) Matsuura, Y., Takano, T., and Dickerson, R. E. (1982) Structure of cytochrome c_{551} from *Pseudomonas aeruginosa* refined at 1.6 Å resolution and comparison of the two redox forms. *J. Mol. Biol. 156*, 389–409.

(18) Takahashi, Y., Sasaki, H., Takayama, S. J., Mikami, S., Kawano, S., Mita, H., Sambongi, Y., and Yamamoto, Y. (2006) Further enhancement of the thermostability of *Hydrogenobacter thermophilus* cytochrome c_{552}. *Biochemistry 45*, 11005–11011.

(19) Lojou, E., and Bianco, P. (2000) Membrane electrodes can modulate the electrochemical response of redox potentials − Direct electrochemistry of cytochrome *c*. *J. Electroanal. Chem. 485*, 71–80.

(20) Takayama, S. J., Takahashi, Y., Mikami, S., Irie, K., Kawano, S., Yamamoto, Y., Hemmi, H., Kitahara, R., Yokoyama, S., and Akasaka, K. (2007) Local conformational transition of *Hydrogenobactor thermophilus* cytochrome c_{552} relevant to its redox potential. *Biochemistry 46*, 9215–9224.

(21) Battistuzzi, G., Borsari, M., Loschi, L., Menziani, M. C., De Rienzo, F., and Sola, M. (2001) Control of metalloprotein reduction potential: The role of electrostatic and solvation effects probed on plastocyanin mutants. *Biochemistry 40*, 6422–6430.

(22) Piotte, M., Saudek, V., and Sklená, V. (1992) Gradient-tailored excitation for single-quantum NMR spectroscopy of aqueous solutions. *J. Biol. NMR 2*, 661–665.

(23) La Mar, G. N., Satterlee, J. D., and de Ropp, J. S. (2000) Nuclear magnetic resonance of hemoproteins, in *The Porphyrin Handbook* (Kadish, K., Smith, K. M., and Guilard, R., Eds.) pp 185−298, Academic Press, New York.

(24) Bertini, I., and Luchinat, C. (1986) *NMR of Paramagnetic Molecules in Biological Systems*, pp 19−46, The Benjamin/Cummings Publishing Company, Menlo Park, CA.

(25) Yamamoto, Y. (1998) NMR study of active sites in paramagnetic hemoproteins. *Ann. Rep. NMR Spectrosc. 36*, 1–77.

(26) Tai, H., Mikami, S., Irie, K., Watanabe, N., Shinohara, N., and Yamamoto, Y. (2010) Role of a highly conserved electrostatic interaction on the surface of cytochrome *c* in control of the redox function. *Biochemistry 49*, 42–48.

(27) Tachiiri, N., Hemmi, H., Takayama, S. J., Mita, H., Hasegawa, J., Sambongi, Y., and Yamamoto, Y. (2004) Effects of axial methionine coordination on the in-plane asymmetry of the heme electronic structure of cytochrome *c*. *J. Biol. Inorg. Chem. 9*, 733–742.

(28) Shokhirev, N. V., and Walker, F. A. (1998) The effect of axial ligand plane orientation on the contact and pseudocontact shifts of low-spin ferriheme proteins. *J. Biol. Inorg. Chem. 3*, 581–594.

(29) Shokhirev, N. V., and Walker, F. A. (1998) Co- and counter-rotation of magnetic axes and axial ligands in low-spin ferriheme systems. *J. Am. Chem. Soc. 120*, 981–990.

(30) La Mar, G. N. (1973) *NMR of Paramagnetic Molecules* (La Mar, G. N., Horrocks, W. D., Jr., and Holm, R. H., Eds.) pp 86−126, Academic Press, New York.

(31) Mikami, S., Tai, H., and Yamamoto, Y. (2010) Effect of the redox-dependent ionization state of the heme propionic acid side chain on the entropic contribution to the redox potential of *Pseudomonas aeruginosa* cytochrome c_{551}. *Biochemistry 49*, 42–48.

(32) Banci, L., Bertini, I., Huber, J. G., Spyroulias, G. A., and Turano, P. (1999) Solution structure of reduced horse heart cytochrome *c*. *J. Biol. Inorg. Chem. 4*, 21–31.

(33) Battistuzzi, G., Borsari, M., Ronieri, A., and Sola, M. (2004) Solvent-based deuterium isotope effects on the redox thermodynamics of cytochrome *c*. *J. Biol. Inorg. Chem. 9*, 781–781.

(34) Battistuzzi, G., Borsari, M., Ronieri, A., and Sola, M. (2002) Redox thermodynamics of the Fe^{3+}/Fe^{2+} couple in horseradish peroxidase and its cyanide complex. *J. Am. Chem. Soc. 124*, 26–27.

(35) Sola, M, Battistuzzi, G., and Borsari, M. (2005) Modulation of the free energy of reduction in metalloproteins. *Chemtracts-Inorg. Chem. 18*, 73–86.